

Deployment of a Cable-Supported Payload from an Orbiting Spacecraft

Thomas R. Kane* and David A. Levinson†
Stanford University, Stanford, Calif.

This paper deals with a passive procedure for bringing a payload connected to an orbiting spacecraft by a cable into a permanent locally vertical position. The procedure consists of placing the cable (except for its end-points) outside of the spacecraft and then ejecting the payload, which thereupon performs a freeflight until the cable becomes taut, at which time the motion is altered drastically and a new freeflight begins. Impacts and freeflights thereafter occur alternately until the cable becomes permanently taut, which marks the beginning of the final deployment phase, during which the payload, acting like a damped spherical pendulum, settles into a locally vertical equilibrium position. An algorithm for simulating the entire deployment sequence is developed, and an illustrative example indicates that the proposed scheme enables one to bring a payload attached with a 100-m-long cable to a spacecraft in a 90-min orbit into a vertically downward position in less than 78 min.

Introduction

AS part of the NASA Gemini program, a successful attempt was made to fly two cable-connected bodies, a modified Agena vehicle and a Gemini capsule, in a gravity-stabilized, Earth-pointing attitude.¹ Previously, this idea had received considerable attention in the spaceflight literature, and it is central presently to a number of mission proposals for the Shuttle, such as Project Skyhook,² which involves placing a satellite in the upper atmosphere of the Earth by attaching the satellite with a long cable to a Shuttle in orbit at a greater altitude. Another application, proposed by Sutton and Diederich,³ is to use these means to produce a satellite that remains above an Earth-fixed point at an altitude either less than or greater than that required for a single-body satellite of this kind.

In the numerous analyses of cable-connected spacecraft performed to date, attention has been focused primarily on postdeployment behavior. Differences between various investigations arise mainly in the modeling of the cable, such as treating it as massless,⁴⁻¹¹ massive,¹²⁻¹⁶ rigid,¹⁷⁻²⁷ or springlike.²⁸⁻³³ The problem of deployment, which was examined briefly by Ebner,³⁴ Chobotov,³⁵ and Kulla,³⁶ obviously deserves attention, for it must be solved in order to render any postdeployment study practically meaningful. Moreover, it does not appear to possess a simple solution.

The present paper deals with a passive deployment procedure, that is, one not requiring actuators to control payload motions. (The aforementioned Gemini experiment involved the use of capsule thrusters during deployment.) The procedure is initiated by placing the cable (except for its endpoints) outside of an orbiting spacecraft, thus causing it to "float" freely. Next, the payload attached to one end of the cable is ejected from the spacecraft and performs a freeflight until the cable becomes taut, at which time the payload is subjected to an impact that alters its motion drastically, whereupon a new free flight begins. Impacts and free flights then occur alternately until so much energy has been dissipated during impacts that no further ones occur and the cable becomes permanently taut. This time marks the beginning of the final phase of deployment, which consists of the motion of a damped spherical pendulum that ultimately settles into one of two stable positions,³⁷ namely, vertically upward or downward. Our goal is to provide the analytical basis for an initial assessment of this concept.

The sequel begins with a description of the system to be analyzed. Next, equations governing free flight, impact, and spherical pendulum motions are presented, and an experimental investigation, carried out to test the assumptions underlying the derivation of the impact equations, is discussed. Finally, a complete deployment analysis algorithm is described, and results obtained by using it are presented.

System Description

In Fig. 1, C designates a light cable of length L which connects a particle P of mass M to particle Q whose mass greatly exceeds M and which is moving at a constant orbital rate Ω on a circular path centered at a point O representing a center of gravitational attraction. The path of Q is presumed to be fixed in a Newtonian reference frame, and a_1, a_2, a_3 are unit vectors, a_1 pointing radially outward, a_2 pointing in the direction of motion of Q , and a_3 being defined as $a_3 \triangleq a_1 \times a_2$.

Free Flight

When C is slack, the motion of P in a reference frame A in which Q and a_i ($i=1,2,3$) are fixed can be described conveniently in terms of functions $x_i(t)$, defined as $x_i(t) \triangleq r \cdot a_i$ ($i=1,2,3$), where r is the position vector of P relative to Q (Fig. 1); and, if $x_i(0)$ and $\dot{x}_i(0)$ denote, respectively, the values of x_i and of the first time-derivative of x_i at $t=0$, then, so long as the distance between P and Q is much smaller than that between O and Q , $x_1(t), x_2(t), x_3(t)$ are given by⁴

$$x_1(t) = [4\Omega x_1(0) + 2\dot{x}_2(0) - [2\dot{x}_2(0) + 3\Omega x_1(0)] \cos \Omega t + \dot{x}_1(0) \sin \Omega t] \Omega^{-1} \quad (1)$$

$$x_2(t) = [\Omega x_2(0) - 2\dot{x}_1(0) - 3\Omega [\dot{x}_2(0) + 2\Omega x_1(0)] t + [4\dot{x}_2(0) + 6\Omega x_1(0)] \sin \Omega t + 2\dot{x}_1(0) \cos \Omega t] \Omega^{-1} \quad (2)$$

$$x_3(t) = [\Omega x_3(0) \cos \Omega t + \dot{x}_3(0) \sin \Omega t] \Omega^{-1} \quad (3)$$

(Equation (3) does not appear in Ref. 4 but can be derived by the same procedures used there.)

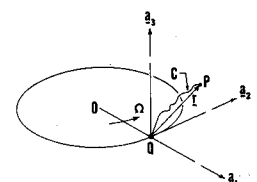


Fig. 1 Spacecraft (Q) and payload (P).

Received Nov. 1, 1976; revision received Feb. 14, 1977.

Index category: Spacecraft Navigation, Guidance, and Flight-Path Control.

*Professor of Applied Mechanics.

†Research Associate.

Impact

Equations (1-3) apply until the instant at which C becomes taut. This instant corresponds to the smallest value of \bar{t} such that

$$\dot{x}_1^2(\bar{t}) + \dot{x}_2^2(\bar{t}) + \dot{x}_3^2(\bar{t}) = L^2 \quad (4)$$

At this instant, P is subjected to an impact which, we shall assume, alters the velocity of P in A in a very short time interval but does not affect its position. To describe the change in velocity we let v and \hat{v} denote, respectively, the velocity of P in A immediately prior and subsequent to impact and write

$$v = -e v \cdot \lambda \lambda + \lambda \times (v \times \lambda) \quad (5)$$

where e is a constant (called the coefficient of restitution), $0 < e < 1$, and λ is a unit vector parallel to line $Q-P$ at the instant of impact. In other words, we assume that the component of \hat{v} parallel to C (recall that C is now straight) has a direction opposite to that of the component of v parallel to C , that the magnitude of the former component is equal to e times that of the latter, and that the components of \hat{v} and v perpendicular to C are equal to each other.

Scalar equations equivalent to Eq. (5) are obtained by defining v_i , \hat{v}_i , and λ_i as $v_i \triangleq v \cdot a_i$, $\hat{v}_i \triangleq \hat{v} \cdot a_i$, and $\lambda_i \triangleq \lambda \cdot a_i$ ($i = 1, 2, 3$), which leads to

$$\hat{v}_1 = -E\lambda_1 + \lambda_2(v_1\lambda_2 - v_2\lambda_1) - \lambda_3(v_3\lambda_1 - v_1\lambda_3) \quad (6)$$

$$\hat{v}_2 = -E\lambda_2 + \lambda_3(v_2\lambda_3 - v_3\lambda_2) - \lambda_1(v_1\lambda_2 - v_2\lambda_1) \quad (7)$$

$$\hat{v}_3 = -E\lambda_3 + \lambda_1(v_3\lambda_1 - v_1\lambda_3) - \lambda_2(v_2\lambda_3 - v_3\lambda_2) \quad (8)$$

where E is defined as

$$E \triangleq e(v_1\lambda_1 + v_2\lambda_2 + v_3\lambda_3) \quad (9)$$

and λ_i and v_i can be found by using Eqs. (1-3), that is,

$$\lambda_i = x_i(\bar{t})/L \quad (i = 1, 2, 3) \quad (10)$$

$$v_1 = [2\dot{x}_2(0) + 3\Omega x_1(0)]\sin\Omega\bar{t} + \dot{x}_1(0)\cos\Omega\bar{t} \quad (11)$$

$$v_2 = -3[\dot{x}_2(0) + 2\Omega x_1(0)] + [4\dot{x}_2(0) + 6\Omega x_1(0)] \times \cos\Omega\bar{t} - 2\dot{x}_1(0)\sin\Omega\bar{t} \quad (12)$$

$$v_3 = -\Omega x_3(0)\sin\Omega\bar{t} + \dot{x}_3(0)\cos\Omega\bar{t} \quad (13)$$

To test the validity of the assumptions expressed by Eq. (5), experiments were performed as follows. A small, shiny object P (Fig. 2) was attached to one end of a string C of length L , the other end of which was fastened to a rigid stand S that was placed in front of a black background B , and a camera was positioned in front of this apparatus. Time exposures then were made to obtain pictures of the path traced out by P subsequent to being released from rest in various positions in the X_1-X_2 plane, and each such path could be compared with its theoretical counterpart generated by using Eqs. (4 and 6-10) to deal with impact, but replacing Eqs. (1-3 and 11-13) with

$$x_1 = x_1(0) + \dot{x}_1(0)t + gt^2/2$$

$$x_2 = x_2(0) + \dot{x}_2(0)t$$

$$x_3 = 0$$

and

$$v_1 = \dot{x}_1(0) + g\bar{t}$$

$$v_2 = \dot{x}_2(0)$$

$$v_3 = 0$$

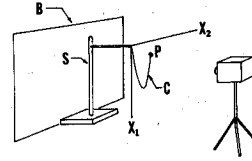


Fig. 2 Experimental apparatus.

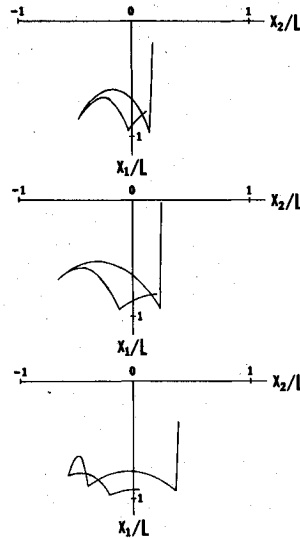


Fig. 3 Experimental results.

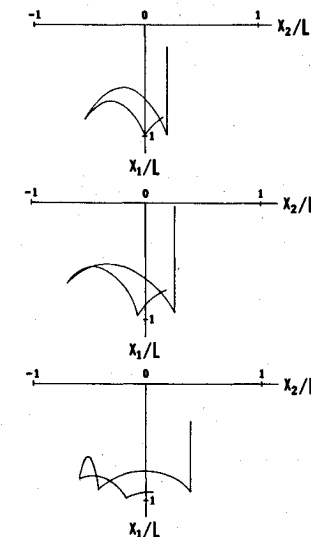


Fig. 4 Theoretical results.

respectively, where g is the local gravitational acceleration. Figure 3 shows tracings made from photographic records for three runs corresponding to different release positions, and the corresponding theoretical curves, for $e = 0.8$, appear in Fig. 4. Clearly, the agreement between theoretical and experimental results is quite good.

Spherical Pendulum Motion

The time interval between successive impacts eventually becomes so small that one may regard C as taut for all subsequent time. (This situation is analogous to that of a bouncing ball, which stops bouncing after a finite time.) Equations (1-3 and 6-10) then no longer apply, the first three because they fail to reflect the force exerted on P by C , and the last seven because they deal solely with impact. Moreover, P then possesses only two degrees of freedom in A , so that it becomes inexpedient to describe the position of P in A in terms of x_1 , x_2 , x_3 . Instead, it is convenient to employ two angles, θ and φ , defined as follows. Let c_1 , c_2 , c_3 be a dextral triad of mutually perpendicular unit vectors, with c_1 parallel

to C and pointing from Q to P , and imagine that P has been brought to a generic position by aligning c_i with a_i ($i=1,2,3$) and then subjecting the triad c_1, c_2, c_3 to successive right-handed rotations of amounts θ about c_2 and φ about c_3 relative to A . This can always be done, and these angles are particularly well suited to the analysis of motions such that C departs but little from line $O-Q$.

One more topic requires consideration before equations governing θ and φ can be formulated. In order for C to approach alignment with $O-Q$, that is, for the pendulum to settle into one of its positions of dynamic equilibrium, rather than to continue moving in A forever, a damping mechanism must be provided. We shall assume that this is done in such a way that, at least when C is nearly in line with $O-Q$, C (now regarded as rigid) is subjected to the action of a couple whose moment M is given by

$$M = -(\alpha\dot{\theta}a_2 + \beta\dot{\varphi}a_3) \quad (14)$$

where α and β are positive constants. (Such a damper can be constructed, perhaps, by attaching C to a small sphere that is embedded in a spherical housing centered at Q and containing a viscous fluid separating the sphere from the housing.)

For large values of θ and φ , the differential equations governing these variables are coupled and complicated. But they possess the exact solutions $\varphi=0, \theta=0$ (P outside the orbit of Q) and $\varphi=0, \theta=\pi$ (P inside the orbit of Q); and, when φ is small and θ is either small or nearly equal to π , they uncouple and reduce to

$$\ddot{\theta} + (\alpha/ML^2)\dot{\theta} + 4\Omega^2\theta \approx \begin{cases} 0 \\ 4\Omega^2\pi \end{cases} \quad (15)$$

$$\ddot{\varphi} + (\beta/ML^2)\dot{\varphi} + 3\Omega^2\varphi \approx 0 \quad (16)$$

In other words, the spherical pendulum motion then is governed by the equations of two damped harmonic oscillators that are critically damped if $\alpha=4ML^2\Omega$ and $\beta=2\sqrt{3}ML^2\Omega$. For these values of α and β , the solutions of Eqs. (15) and (16) are

$$\theta(t) \approx \begin{cases} (at+b)\exp(-2\Omega t) \\ \pi + (at+b)\exp(-2\Omega t) \end{cases} \quad (17)$$

$$\varphi(t) \approx (ct+d)\exp(-\sqrt{3}\Omega t) \quad (18)$$

where a, \dots, d are constants whose values must be chosen such that the position and velocity of P in A at the beginning of spherical pendulum motion match those at the end of the last impact. To determine these values, note first that, from Eq. (17),

$$a = \begin{cases} 2\Omega\theta(0) + \dot{\theta}(0) \\ 2\Omega[\theta(0) - \pi] + \dot{\theta}(0) \end{cases} \quad b = \begin{cases} \theta(0) \\ \theta(0) - \pi \end{cases} \quad (19)$$

while, from Eq. (18),

$$c = \sqrt{3}\Omega\varphi(0) + \dot{\varphi}(0) \quad d = \varphi(0) \quad (20)$$

Next, recall that r , the position vector of P relative to Q , can be expressed, for all t , as $r = x_1a_1 + x_2a_2 + x_3a_3$ and, when C is taut, as $r = Lc_i$. Additionally, when C is nearly aligned with $O-Q$,

$$C_i \approx \begin{cases} a_1 + \varphi a_2 - \theta a_3 \\ -a_1 + \varphi a_2 + (\theta - \pi)a_3 \end{cases} \quad (21)$$

Consequently, one then has

$$x_1 \approx \begin{cases} L \\ -L \end{cases} \quad x_2 \approx L\varphi \quad x_3 \approx \begin{cases} -L\theta \\ L(\theta - \pi) \end{cases} \quad (22)$$

and, by differentiation,

$$\dot{x}_1 \approx 0 \quad \dot{x}_2 \approx L\dot{\varphi} \quad \dot{x}_3 \approx \begin{cases} -L\dot{\theta} \\ L\dot{\theta} \end{cases} \quad (23)$$

Hence, if we designate as $t=0$ the instant at which pendulum motion begins, and let \bar{x}_i and \bar{v}_i denote respectively the values of x_i and v_i at this instant, then Eqs. (22) and (23) permit us to write

$$\theta(0) \approx \begin{cases} -\bar{x}_3/L \\ \pi + \bar{x}_3/L \end{cases} \quad \dot{\theta}(0) \approx \begin{cases} -\bar{v}_3/L \\ \bar{v}_3/L \end{cases} \quad (24)$$

and

$$\varphi(0) \approx \bar{x}_2/L \quad \dot{\varphi}(0) \approx \bar{v}_2/L \quad (25)$$

whereupon substitution into Eqs. (19) and (20) yields

$$a = \begin{cases} -(\bar{v}_2 + 2\Omega\bar{x}_2)/L \\ (\bar{v}_2 + 2\Omega\bar{x}_2)/L \end{cases} \quad b = \begin{cases} -\bar{x}_3/L \\ \bar{x}_3/L \end{cases} \quad (26)$$

and

$$c = (\bar{v}_2 + \sqrt{3}\Omega\bar{x}_2)/L \quad d = \bar{x}_2/L \quad (27)$$

Deployment Analysis Algorithm

Recapitulating, we note that the algorithm now to be described is intended to enable one to accomplish the following. Given the orbital rate Ω , the payload mass M , the cable length L , the coefficient of restitution e , and payload ejection conditions, that is, $x_i(0)$ and $\dot{x}_i(0)$ ($i=1,2,3$), intended to bring the payload to rest ultimately on line $O-Q$, either outside of the orbit of Q ($\theta=0, \varphi=0$) or inside ($\theta=\pi, \varphi=0$), determine whether or not the desired goal can be attained in a reasonable time, and, if so, describe the entire deployment in detail.

Computations are begun by using Eqs. (1-4) and a root-finder to discover the time \bar{t} and the associated values $x_i(\bar{t})$ of x_i ($i=1,2,3$) for the first impact. Next, λ_i, v_i , and \bar{v}_i ($i=1,2,3$) are determined by means of Eqs. (10, 11-13, and 6-9), respectively, after which the first step is repeated with $x_i(\bar{t})$ and \bar{v}_i in place of $x_i(0)$ and $\dot{x}_i(0)$, respectively. This process is continued until \bar{t} has become smaller than a preassigned small value, say 0.01 sec, at which point \bar{x}_i and \bar{v}_i are formed by setting them equal to the most recent values of x_i and \dot{x}_i ($i=1,2,3$), respectively; $\theta(0)$ and $\varphi(0)$ are evaluated by reference to Eqs. (24) and (25), the upper line in Eq. (24) being used if $\bar{x}_3 > 0$, and the lower if $\bar{x}_3 < 0$; and a test is made to ensure that the absolute values of $\theta(0)$ [or $\theta(0) - \pi$] and $\varphi(0)$ are sufficiently small, say less than 15° , to justify subsequent use of Eqs. (18) and (19). If this is not the case, computations are terminated, not only for analytical reasons but because the "settling" time associated with a pendulum motion that begins with a large angle between C and line $O-Q$ may be expected to be objectionably long. If the test is passed, one proceeds to the evaluation of a, \dots, d by means of Eqs. (26) and (27), and $\theta(t)$ and $\varphi(t)$ then are found for a succession of values of t by using Eqs. (17) and (18). Here it is necessary to test θ and φ periodically, for it may occur that C departs markedly from $O-Q$ subsequent to $t=0$. Finally, computations are concluded when the absolute values of θ (or $\theta - \pi$) and φ have become smaller than a preassigned small value, say 1° .

Turning to an illustrative example, we take $\Omega = \pi/2700$ rad/sec, $M = 1$ kg, $L = 100$ m, and $e = 0.2$ and explore the

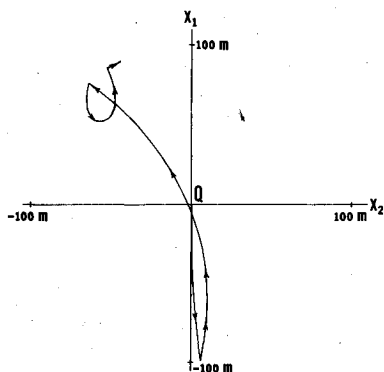


Fig. 5 Unsuccessful deployment attempt.

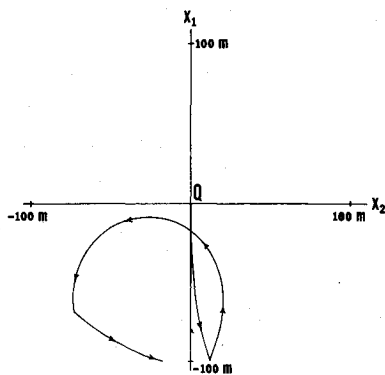


Fig. 6 Successful deployment.

possibility of deploying P to the inside of the orbit of Q by letting $x_i(0) = 0$ ($i = 1, 2, 3$), $\dot{x}_i(0) = -2$ m/sec, and $\dot{x}_2(0) = \dot{x}_3(0) = 0$, these values reflecting the admittedly naive notion that it may suffice simply to fire the payload toward the target. Proceeding as required, we find that the first impact occurs after 49.94 sec, at which time $x_1 = -99.83$ m, $x_2 = 5.80$ m, $x_3 = 0$, and that the velocity of P in reference frame A at this instant is described by $\dot{v}_1 = -2.00$ m/sec, $\dot{v}_2 = 0.23$ m/sec, $\dot{v}_3 = 0$. The second free flight consumes 531.12 sec, the third 918.50 sec, the fourth 132.36 sec, the fifth 24.57 sec, and the sixth less than 0.01 sec. Hence we regard the cable as permanently taut subsequent to the sixth impact, which takes place at $x_1 = 89.26$ m, $x_2 = -45.09$ m, $x_3 = 0$, these thus being the values of \bar{x}_1 , \bar{x}_2 , \bar{x}_3 , respectively. Since $\bar{x}_1 > 0$, it is clear that we are, at best, on the way to an outside, rather than the desired inside, deployment. Moreover, Eqs. (24) and (25) yield $\theta = 0$ rad, $\varphi = -0.45$ rad, the latter of which is too large to permit the use of Eq. (18). Hence we terminate the computations. The trajectory of P in A during the free flights of this unsuccessful deployment attempt is shown in Fig. 5, which reveals yet one more flaw of the motion under consideration— P comes to close to Q (within 1 m) during the second free flight.

By way of contrast, Fig. 6 illustrates a successful attempt to achieve inward deployment. Here, all parameters have the same values as before, $x_i(0)$ ($i = 1, 2, 3$) and \dot{x}_i ($i = 2, 3$) again are equal to zero, but $\dot{x}_1(0) = -1$ m/sec, that is, one-half of the value used previously. The first 10 free flights now last for a total of 1880.08 sec, the last one taking 0.003 sec; $\bar{x}_1 = -98.58$ m, $\bar{x}_2 = -16.77$ m, $\bar{x}_3 = 0$; $\dot{v}_1 = -0.034$ m-sec $^{-1}$, $\dot{v}_2 = 0.20$ m-sec $^{-1}$, $\dot{v}_3 = 0$; $\bar{x}_1 < 0$, as desired; and $\theta(0) = \pi$, whereas $\varphi(0) = -0.168$ rad, so that we may proceed to the evaluation of a, \dots, d , which yields $a = b = 0$, $c = 0.0017$ sec $^{-1}$, $d = -0.168$, after which Eqs. (17) and (18) reveal that $\theta = \pi$, whereas φ never exceeds 15° and decays to less than 1° within 47 min of the beginning of the pendulum motion.

The durations of the free flight and pendulum motion phases are relatively insensitive to rather substantial changes in the values of e , α , and β . For example, reductions of 5, 10, 15, and 20% in the value of e result in respective decreases of

only 1.6, 1.4, 2.0, and 4.2% in the total free flight time; and numerical integrations of the full nonlinear spherical pendulum equations of motion reveal that simultaneously halving α and β increases by only 12 min the time required for φ to decay to less than 1° , whereas reducing α and β to 25% of their original values increases the decay time to 132 min, which is less than the time required by the spacecraft to complete one and one-half orbits.

Conclusion

The deployment analysis algorithm under consideration does not lead to exact results, partly because mathematical approximations, such as linearizations, were made in deriving some of the equations on which it is based and, more importantly, because two major physical assumptions were made in the course of the analysis, namely, that cable mass can be neglected and that a damper acting in accordance with Eq. (14) can be constructed. Nevertheless, this work furnishes a clear indication that the proposed deployment scheme holds promise, and thus it provides the motivation for more refined analyses.

Acknowledgment

This work was supported by the National Foundation under Grant NSF-ENG-75-18680 to Stanford University.

References

- Lang, D.D. and Nolting, R.K., "Operations with Tethered Vehicles," *Gemini Summary Conference*, NASA SP-138, Feb. 1-2, 1967, pp. 55-64.
- Colombo, G., Gaposchkin, E.M., Grossi, M.D., and Weiffenbach, G.C., "Shuttle-Borne 'Skyhook': A New Tool for Low-Orbital-Altitude Research," *Smithsonian Institution Astrophysical Observatory Rept.*, Sept. 1974.
- Sutton, G.W. and Diederich, F.W., "Synchronous Rotation of a Satellite at Less than Synchronous Altitude," *AIAA Journal*, Vol. 5, April 1967, pp. 813-815.
- Adams, W. M. Jr., "Dynamics of Two Slowly Rotating Point-Mass Vehicles Connected by a Massless Tether and in a Circular Orbit," *NASA TN D-5599*, Jan. 1970.
- Stabekis, P. and Bainum, P. M., "Motion and Stability of a Rotating Space Station-Cable-Counterweight Configuration," *Journal of Spacecraft and Rockets*, Vol. 7, Aug. 1970, pp. 912-918.
- Novikova, E.T., "Can There Be Steady Rotation of a Group of Connected Bodies in Orbit?," *Moscow University Mechanics Bulletin*, Vol. 29, May 1974, pp. 88-90.
- Austin, F., "Equations of Motion for a Rotating Cable Connected Space Station," *Grumman Aircraft Engineering Corp.*, Interoffice Memo. STMECH 69.54, June 1969.
- Childs, D.W. and Hardison, T.L., "A Movable-Mass Attitude Stabilization System for Cable-Connected Artificial-g Space Stations," *Journal of Spacecraft and Rockets*, Vol. 11, March 1974, pp. 165-172.
- Bainum, P.M. and Evans, K.S., "Three-Dimensional Motion and Stability of Two Rotating Cable-Connected Bodies," *Journal of Spacecraft and Rockets*, Vol. 12, April 1975, pp. 242-250.
- Beletskii, V.V. and Novikova, E.E., "Relative Motion of a Link-Up of Two Objects in Orbit," *Kosmicheskie Issledovaniya*, Vol. 7, May-June 1969, pp. 377-384.
- Singh, R.B., "Three Dimensional Motion of a System of Two Cable-Connected Satellites in Orbit," *Astronautica Acta*, Vol. 18, Nov. 1973, pp. 301-308.
- Kerr, W.C. and Abel, J.M., "Transverse Vibrations of a Rotating Counterweighted Cable of Small Flexural Rigidity," *AIAA Journal*, Vol. 9, Dec. 1971, pp. 2326-2332.
- Chobotov, V., "Gravity-Gradient Excitation of a Rotating Cable-Counterweight Space Station in Orbit," *American Society of Mechanical Engineers Paper 63-APMW-16*, 1963.
- Anderson, W.W., "On Lateral Cable Oscillations of Cable-Connected Space Stations," *NASA TN D-5107*, 1968.
- Tai, C.L. and Loh, M.M.H., "Planar Motion of a Rotating Cable-Connected Space Station in Orbit," *Journal of Spacecraft and Rockets*, Vol. 2, Nov.-Dec. 1965, pp. 889-894.
- Garber, T.B., "A Preliminary Investigation of the Motion of a Long, Flexible Wire in Orbit," *Rand Corp. Rept. RM-2705-ARPA*, March 23, 1961.

¹⁷Schechter, H.B., "Dumbbell Librations in Elliptic Orbits," *AIAA Journal*, Vol. 2, June 1964, pp. 1000-1003.

¹⁸Robinson, W.J., "The Restricted Problem of Three Bodies with Rigid Dumb-Bell Satellite," *Celestial Mechanics*, Vol. 8, Sept. 1973, pp. 323-330.

¹⁹Pisacane, V.L., "Three-Axis Stabilization of a Dumbbell Satellite by a Small Constant-Speed Rotor," Johns Hopkins Univ., Applied Physics Lab., Tech. Mem. TG-855, Oct. 1966.

²⁰Ordway, D.E., "Coupled Planar Motion of a Dumbbell Satellite," Therm Advanced Research Rept. TAR-TN 611, June 1961.

²¹Ikunev, Yu. M., "Possible Motions of a Long Dumbbell in a Central Force Field," *Kosmicheskie Issledovaniya*, Vol. 7, May 1969, pp. 637-642.

²²Klemperer, W.B., "Satellite Librations," *Navigation*, Vol. 6, Spring 1958, pp. 62-63.

²³Brereton, R.C. and Modi, V.J., "On the Stability of Planar Librations of a Dumb-bell Satellite in an Elliptic Orbit," *Journal of the Royal Aeronautical Society*, Vol. 70, Dec. 1966, pp. 1098-1102.

²⁴Saeed, I. and Stuver, W., "Periodic Boom Forces in Dumbbell-Type Satellites," *AIAA Journal*, Vol. 12, April 1974, pp. 425-426.

²⁵Garber, T.B., "A Semi-Passive, Three-Axis Stabilization Technique for Dumbbell-Type Satellites," Rand Corp., Oct. 1968.

²⁷Moran, J.P., "Effects of Plane Librations on the Orbital Motion of a Dumbbell Satellite," *ARS Journal*, Vol. 31, 1961, pp. 1089-1096.

²⁸Pringle, R. Jr., "Exploitation of Nonlinear Resonance in Damping an Elastic Dumbbell Satellite," *AIAA Journal*, Vol. 6, July 1968, pp. 1217-1222.

²⁹Pitman, D.L. and Hall, B.M., "The Inherent Stability of Counterweight Cable Connected Space Stations," Douglas Missile & Space Systems Div., Paper 3501, July 1964.

³⁰Austin, F., "Nonlinear Dynamics of a Free-Rotating Flexibly Connected Double-Mass Space Station," *Journal of Spacecraft and Rockets*, Vol. 2, Nov.-Dec. 1965, pp. 901-906.

³¹Crist, S.A. and Easley, J.G., "Cable Motion of a Spinning Spring-Mass System in Orbit," *Journal of Spacecraft and Rockets*, Vol. 7, Nov. 1970, pp. 1352-1357.

³⁴Ebner, S.G., "Deployment Dynamics of Rotating Cable-Connected Space Stations," *Journal of Spacecraft and Rockets*, Vol. 7, Oct. 1970, pp. 1274-1275.

³⁵Chobotov, V.A., "Synchronous Satellite at Less Than Synchronous Altitude," *Journal of Spacecraft and Rockets*, Vol. 13, Feb. 1976, pp. 126-128.

³⁶Kulla, P., "Dynamics of Tethered Satellites," *Proceedings of the Symposium on the Dynamics and Control of Non-Rigid Spacecraft*, European Space Agency, Frascati, Italy, May 1976, pp. 349-354.

³⁷Synge, J.L., "On the Behaviour According to Newtonian Theory, of a Plumb Line or Pendulum Attached to an Artificial Satellite," *Proceedings of the Royal Irish Academy*, Vol. 60, Sec. A, Jan. 1959, pp. 1-6.

From the AIAA Progress in Astronautics and Aeronautics Series . . .

INSTRUMENTATION FOR AIRBREATHING PROPULSION—v. 34

Edited by Allen Fuhs, Naval Postgraduate School, and Marshall Kingery, Arnold Engineering Development Center

This volume presents thirty-nine studies in advanced instrumentation for turbojet engines, covering measurement and monitoring of internal inlet flow, compressor internal aerodynamics, turbojet, ramjet, and composite combustors, turbines, propulsion controls, and engine condition monitoring. Includes applications of techniques of holography, laser velocimetry, Raman scattering, fluorescence, and ultrasonics, in addition to refinements of existing techniques.

Both inflight and research instrumentation requirements are considered in evaluating what to measure and how to measure it. Critical new parameters for engine controls must be measured with improved instrumentation. Inlet flow monitoring covers transducers, test requirements, dynamic distortion, and advanced instrumentation applications. Compressor studies examine both basic phenomena and dynamic flow, with special monitoring parameters.

Combustor applications review the state-of-the-art, proposing flowfield diagnosis and holography to monitor jets, nozzles, droplets, sprays, and particle combustion. Turbine monitoring, propulsion control sensing and pyrometry, and total engine condition monitoring, with-cost factors, conclude the coverage.

547 pp. 6 x 9, illus. \$14.00 Mem. \$20.00 List

TO ORDER WRITE: Publications Dept., AIAA, 1290 Avenue of the Americas, New York, N. Y. 10019